https://doi.org/10.5194/acp-2020-827
Preprint. Discussion started: 25 August 2020

Atmospheric Chemistry and Physics
Discussions

Wildfire smoke-plume rise: a simple energy balance parameterization

Nadya Moisseeva[1] and Roland Stull[1]

[1]Department of Earth, Ocean and Atmospheric Sciences, The University of British Columbia, Vancouver BC V6T 1Z4, Canada

Correspondence: Nadya Moisseeva (nmoisseeva@eoas.ubc.ca)

Abstract. The buoyant rise and the resultant vertical distribution of wildfire smoke in the atmosphere have a strong influence on downwind pollutant concentrations at the surface. The amount of smoke injected vs. height is a key input into chemical transport models and smoke modelling frameworks. Due to scarcity of model evaluation data as well as inherent complexity of wildfire plume dynamics, smoke injection height predictions have large uncertainties. In this work we use a coupled fire-atmosphere model WRF-SFIRE configured in large eddy simulation (LES) mode to develop a synthetic plume dataset. Using this numerical data, we demonstrate that crosswind integrated smoke injection height for a fire of arbitrary shape and intensity can be modelled with a simple energy balance. We introduce two forms of updraft velocity scales that exhibit a linear dimensionless relationship with the plume vertical penetration distance through daytime convective boundary layers. Lastly, we use LES and prescribed burn data to constrain and evaluate the model. Our results suggest that the proposed simple parameterization of mean plume rise as a function of vertical velocity scale offers reasonable accuracy (30 m errors) at little computational cost.

1 Introduction

Predictions of surface concentrations of wildfire smoke by regional and global chemical transport models depends on the initial equilibrium height of the smoke plume. Plume rise, which determines this equilibrium height, is widely recognized as an area of uncertainty (Goodrick et al., 2013; Paugam et al., 2016). Traditionally, many operational smoke modelling frameworks relied on plume rise equations originally developed by Briggs (1975) for industrial smokestacks (Larkin et al., 2010; Pavlovic et al., 2016). Yet several studies suggest that this approach may not be appropriate for wildfires (Pavlovic et al., 2016; Heilman et al., 2014; Freitas et al., 2007).

In a recent review of existing plume rise parameterizations, Paugam et al. (2016) highlight three notable models that stand out in literature, as that of Freitas et al. (2007), Sofiev et al. (2012) and Rio et al. (2010). Both Freitas and Rio's approaches use first principles to characterize plume temperature, vertical velocity and entrainment. While the former provides prognostic 1-D equations that can be solved as a stand-alone "offline" model, the latter is implemented as a sub-grid effect within a host chemistry transport model. Notably, both consider an idealized heat source to represent the fire. Sofiev's semi-empirical approach relies on energy balance and dimensional analysis, while using satellite data to both initialize and constrain the

https://doi.org/10.5194/acp-2020-827
Preprint. Discussion started: 25 August 2020

Atmospheric Chemistry and Physics Discussions

parameterization. Unlike Briggs's equations, all of the above models address wildfire plumes specifically, yet much research is needed to reduce the large uncertainties associated with the model predictions (Mallia et al., 2018). Moreover, it is unclear, whether unreliable predictions should be attributed to the fire input parameters or the plume rise model itself.

One of the central challenges in plume rise model development has been the scarcity of comprehensive model evaluation data (Coen et al., 2012b; Ottmar et al., 2016). To date, information on wildfire smoke emissions and dispersion has largely been derived from two distinct sources: remotely sensed data and prescribed burn campaigns. While increasing numbers of satellite observations contribute to a more complete plume climatology (Val Martin et al., 2010), the data is subject to biases and lacks direct spatiotemporal links to fire behavior (Ichoku et al., 2012). In contrast, field campaigns, such as Prescribed Fire Combustion and Atmospheric Dynamics Research Experiment (RxCADRE) (Ottmar et al., 2016) and Fire and Smoke Model Evaluation Experiment (FASMEE) (Prichard et al., 2019), provide the necessary level of detail for model validation studies. However, such datasets typically capture a modest range of fire and atmospheric conditions.

Our approach, therefore, is to develop a synthetic plume dataset that addresses the limitations of the available observational data. As vast majority of smoke plumes remain in or just above the atmospheric boundary layer (ABL) (Val Martin et al., 2010; Mallia et al., 2018), we use large eddy simulations (LES) to focus on local- and meso- scale plume dynamics. Using a coupled model, we simulate a wide range of fire and atmospheric conditions (Sect. 2). Based on this synthetic LES data (hereafter referred to as "data") we propose a simple energy balance model for predicting plume rise of crosswind integrated (CWI) smoke from a non-uniform fireline (Sect. 3). We use the synthetic plume dataset to constrain and evaluate our plume rise parameterization. We then demonstrate with both numerical and prescribed burn data, that within the range of tested conditions this parameterization offers high speed and accuracy (Sect. 4). Our hope is that the proposed smoke plume rise parameterization will help improve smoke dispersion predictions within air quality applications. The ultimate goal is to provide better health and evacuation warnings to communities downwind of wildfires.

2 Development of a Synthetic Plume Dataset

We devise a synthetic plume data set using a coupled fire-atmosphere model WRF-SFIRE, which combines the well-established Weather and Research Forecasting Model (WRF) with a semi-emperical fire spread algorithm called SFIRE (Mandel et al., 2014; Mallia et al., 2018; Coen et al., 2012a; Kochanski et al., 2013; Clements et al., 2006; Kochanski et al., 2019). The following sections detail the numerical setup, scope of the dataset, as well as our approach to defining "ground truth" for model evaluation.

2.1 Numerical Configuration

WRF-SFIRE was configured in idealized large-eddy resolving mode. Much of our numerical setup was adopted from a case study of a real prescribed burn as detailed in Moisseeva and Stull (2019), to ensure the simulations represent physical conditions backed by model evaluation. Due to high computational demands of LES runs, we focused on the local- and meso- scales, considering only the initial buoyant plume rise of smoke in typical daytime atmospheres. Key parameters varied were ambient

https://doi.org/10.5194/acp-2020-827
Preprint. Discussion started: 25 August 2020

Atmospheric Chemistry and Physics Discussions

wind, fuel category, vertical potential temperature profile and fireline length, denoted as conditions **W**,**F**,**R** and **L**, respectively (detailed further in Sect. 2.2).

Each 10 km x 20 km domain with 40 m horizontal grid spacing was initialized with uniform ambient west wind **W** and vertical temperature profile **R**. Depending on the sounding **R**, the simulations were performed in either a shallow (3000 m) or a deep (5000 m) domain, with 51 or 71 hyperbolically stretched vertical levels, respectively. A constant uniform lower boundary surface thermal flux (tke_heat_flux) in the ambient environment and lateral periodic boundary conditions were imposed to produce a turbulent well-mixed layer. We used full surface initialization (sfc_full_init =.true.), with the lower boundary characteristics set to USGS values for land use most closely matching the Anderson fuel category **F** (Anderson, 1982). The corresponding surface roughness lengths added various levels of wind shear to each domain to produce a more realistic non-uniform vertical wind profile during spinup of the environment before the fire was initialized in the LES.

Initial convection in the ambient environment was triggered using a perturbed surface temperature field. On average, a near-stationary turbulence spectrum was achieved within the first 30 min of run start. The "restart" file generated at the end of one hour of spinup was used to initialize the main burn simulation, ensuring the fire was ignited in a well-mixed turbulent ABL.

The fire was initialized over a one-minute interval using a straight line of length **L**. The ignition line was placed one kilometer downwind of the western edge of the domain and centered in the north-south direction. With a refinement ratio of 10 in each horizontal direction, the fire was simulated on a 4 m sub-grid mesh.

The "smoke plume" was modelled with a passive tracer emitted proportionally to the mass and type of fuel burned. The rate of release was controlled by an assigned emission factor representing $PM_{2.5}$ for each fuel category, based on values provided by Prichard et al. (2017) (see namelist.fire_emissions in Supplementary Material).

A summary of key configuration details can be found in Table 1, as well as in sample namelist initialization files provided as Supplementary Material.

2.2 Test Conditions

Table 2 summarizes the key parameters that were varied to produce the synthetic dataset.

The range of ambient winds tested was bound largely by numerical constraints. Due to cyclic boundary conditions, wind speeds higher than 12 $\mathrm{ms^{-1}}$ would require a much larger domain to prevent smoke recirculation. For the lower bound on our wind condition **W**, we needed to ensure that sufficient wind speed was maintained to propagate the fire. The spread algorithm used within the LES applies a correction factor under low wind speed conditions to prevent the fire from extinguishing itself. While necessary for numerical reasons this effect is not physical, so winds below 3 $\mathrm{ms^{-1}}$ were excluded from our dataset.

We used 9 different atmospheric profiles (**R** condition) to initialize the model. We varied the following features for each initialization:

- initial ABL height (500 m - 1600 m)
- potential temperature lapse rate above inversion (0 $\mathrm{K\,km^{-1}}$ - 20 $\mathrm{K\,km^{-1}}$)
- initial ABL temperature (290 K - 300 K)

https://doi.org/10.5194/acp-2020-827
Preprint. Discussion started: 25 August 2020

Atmospheric Chemistry and Physics Discussions

Table 1. Key parameters of numerical domain setup.

Simulation Parameter	**Value/Description**
Model version	May 24, 2019 (git #ced5955)
Horizontal grid spacing	40 m
Domain size	500 grids cells (east-west) x 250 grids cells (north-south)
Time step	0.1 s
Model top	3000 m (shallow) / 5000 m (deep)
Spinup timing	11:30:00 - 12:30:00
Fire (restart) simulation timing	12:30:00 - 12:50:00 (shallow) / 12:30:00 - 13:00:00 (deep)
Sub-grid scale closure	1.5 TKE (TKE = Turbulence kinetic energy)
Lateral boundary conditions	periodic
Surface physics	Monin-Obukhov similarity (sf_sfclay_physics = 1)
Land surface model	thermal diffusion (sf_surface_physics = 1)
Ambient surface heat flux	240 $\mathrm{Wm^{-2}}$(tke_heat_flux=0.2)
Fire mesh refinement	10
Ignition duration	13:00:10 – 13:01:10
Heat of combustion of dry fuel	16.4e+06 J $\mathrm{kg^{-1}}$

Table 2. Test conditions included in synthetic plume dataset. The count indicates the number of unique values used within the specified range.

Condition (Tag)	**Range**	**Count**	**Description**
Ambient wind (W)	3 - 12 $\mathrm{ms^{-1}}$	10	Uniform horizontal wind magnitude used to initialize model spinup
Stability profile (R)	R0-R8	9	Atmospheric sounding with variable ABL height, temperature and inversion strength
Fuel (F)	1 - 13	13	Anderson fuel category assigned at lower boundary
Fireline length (L)	1 - 4 km	3	Length of ignition line
			Total number of experiments = 140

Following spinup (Sect. 2.1) under variable winds and surface conditions, this produced 9 sets of soundings, shown in Fig. 1 with ABL depths of approximately 600 m - 2000 m.

We tested all fuel categories available within the model (**F** condition), and varied the length of the fireline (**L** condition) between 1 and 4 km. Weakly buoyant non-penetrative plumes whose smoke remained within the well-mixed ABL were excluded from the dataset, as their behavior is governed by different physics.

https://doi.org/10.5194/acp-2020-827
Preprint. Discussion started: 25 August 2020

Atmospheric Chemistry and Physics
Discussions

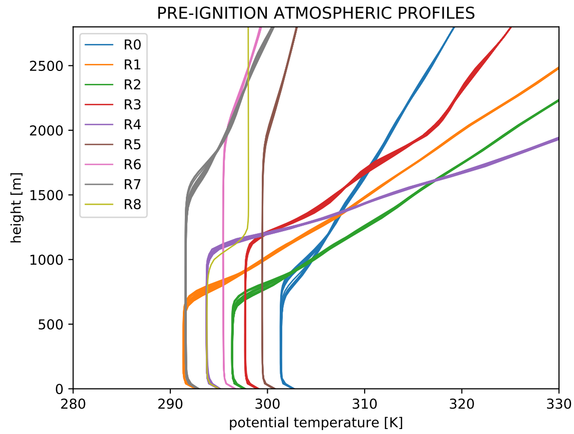

Figure 1. Pre-ignition potential temperature profiles (stability condition **R**). Colors correspond to initial soundings used for model spinup.

Note, that varying a single condition while holding the rest constant does not result in a controlled experiment isolating its impact on plume rise. Because WRF-SFIRE incorporates fire-atmosphere coupling, the problem is not well-constrained. For example, by varying fuel type **F** alone, while holding the rest of test conditions constant, we obtain a set of fires with diverse shapes, sizes, intensities, fireline depths, rates of spread and heat release. This reflects the complexity of non-linear interactions that exist between the fire and the atmosphere. As a result, the parameter space captured within our LES dataset is much greater then the four conditions described in Table 2.

2.3 Defining Smoke Injection Height

Given non-stationary fire and atmospheric conditions, determining a consistent definition of an equilibrium smoke injection height is not a trivial task. It requires separating buoyant rise from dispersion, while excluding the effects of initial momentum overshoot and accounting for the advection due to varying ambient and fire-generated winds.

A common way of examining vertical distributions of pollutants in the context of air quality is to consider CWI concentrations. This allows to reduce the problem to two dimensions, with plume centerline being defined simply as the CWI concentration maximum at each location downwind of the source. Theoretically, under stationary conditions there exists an equilibrium height, around which the centerline eventually oscillates. In reality, as well as in our LES experiments, neither the ambient nor the fire conditions are stationary. The changing location, shape and intensity of the fire, ABL warming and growth, as well as the development of fire-coupled winds and vorticity continually modify the conditions.

As a result, our approach is based on defining a region, where the concentration distribution is quasi-stationary. We consider the last frame of each simulation for this analysis. Using CWI integrated tracer values, we locate the plume centerline (Fig. 2a). To obtain the quasi-stationary region for each individual plume, we first calculate the change in tracer concentration along the centerline. We then use a smoothing function to reduce the effect of random turbulent oscillations in both the centerline

https://doi.org/10.5194/acp-2020-827
Preprint. Discussion started: 25 August 2020

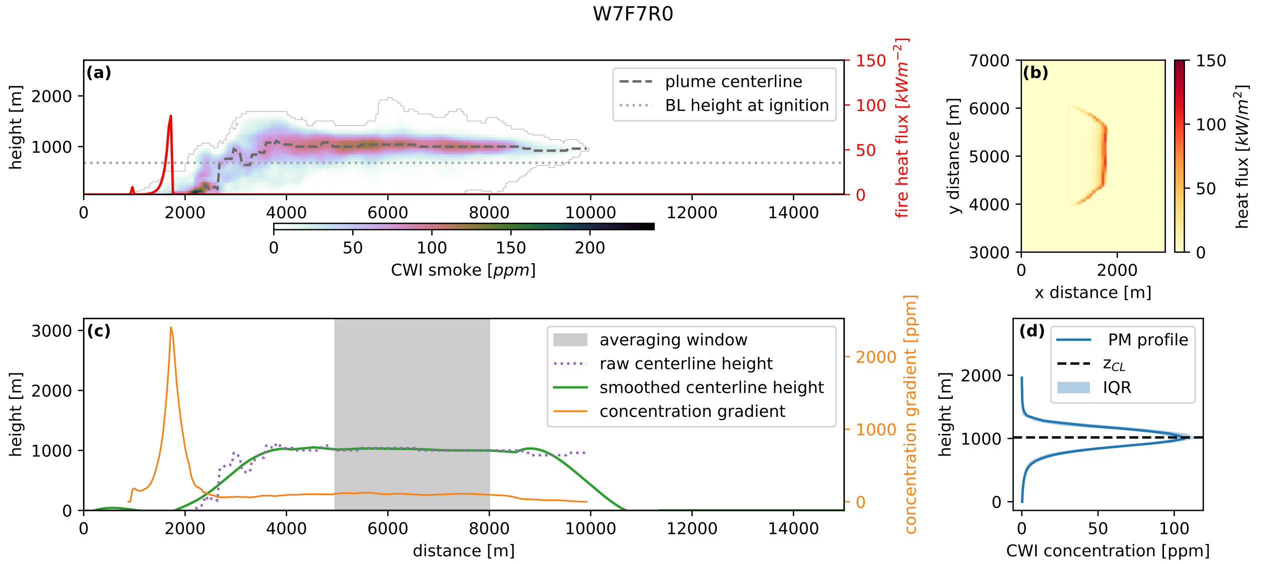

Figure 2. Illustration of the approach to identifying a quasi-stationary downwind region in CWI smoke distribution using a sample LES experiment. (**a**) CWI smoke concentrations. Also shown are plume centerline height (dashed), z_i (dotted) and CWI fireline intensity (solid red, secondary axis). (**b**) Plan view of fire heat flux showing the fireline. (**c**) Quasi-stationary region (grey shading). Also shown are raw (dotted purple) and smoothed (solid green) centerline heights and the tracer concentration gradient (solid orange, secondary axis). (**d**) Representative downwind smoke distribution. The profile (solid blue line) is obtained by horizontally averaging the CWI smoke concentrations in the quasi-stationary region. Also shown are IQR (light blue shading) and the derived smoke injection centerline height z_{CL} (dashed black).

height and the tracer concentration gradient along the centerline. The downwind region where both of these parameters are not changing rapidly are then then considered quasi-stationary. Additional details of this filtering method are provided in Appendix A.

The vertical CWI distribution of tracers are then averaged in the downwind direction over the identified quasi-stationary regions (shaded in grey on the Fig. 2c) to produce a representative downwind distribution for each plume (Fig. 2d). We define the "true" injection height z_{CL} as the mean height of smoothed centerline over the averaging region. The resultant dataset of z_{CL} values is used to constrain and evaluate the proposed smoke injection height parameterization introduced in the following sections.

3 Smoke Injection Height Model for Penetrative Wildfire Plumes

A common approach to predicting the final equilibrium centerline height of wildfire smoke is to first estimate the initial buoyant energy of the hot rising smoke (Briggs, 1975; Sofiev et al., 2012; Anderson et al., 2011). After the smoke plume

https://doi.org/10.5194/acp-2020-827
Preprint. Discussion started: 25 August 2020

entrains surrounding ABL environmental air and cools, the remaining energy is spent doing work to push the cooled smoke plume up into the statically stable capping inversion.

The relationship between final and initial energies is often rewritten to show that the potential energy per unit mass (PE) of smoke penetration equals some fraction c_1 of initial heat released from the fire. In kinematic units, the initial heat input has units similar to a kinetic energy per unit mass (KE). The empirical parameter c_1 is usually estimated based on concepts of entrainment into the rising smoke plume (Cushman-Roisin, 2014).

$$PE = c_1 KE \tag{1}$$

The PE of smoke-plume penetration into the capping inversion can be written as

$$PE = g'z' \tag{2}$$

where the penetration distance z' of the final equilibrium smoke centerline z_{CL} above reference height z_s (near the top of the well-mixed portion of ABL) is

$$z' = z_{CL} - z_s \tag{3}$$

The static-stability variable g' for the plume-penetration region is

$$g' = g\frac{\theta_{CL} - \theta_s}{\theta_s} = g\frac{\theta'}{\theta_s} \tag{4}$$

where θ_{CL} and θ_s are the potential temperatures of the ambient environment at z_{CL} and z_s, respectively, and $\theta_{CL} - \theta_s = \theta'$.

The KE can be estimated using a velocity scale w_f as

$$KE = 0.5 w_f^2 \tag{5}$$

Traditionally, the bulk potential-temperature difference across the smoke-plume penetration region θ' is expected to be relevant for only the PE portion of Eq. (1). However, we found from the LES runs for a wide range of fire and environment conditions that the KE also depends on the same potential temperature difference. This dependence can be expressed in the velocity scale:

$$w_f = \frac{I}{z_i \theta'} \tag{6}$$

This velocity scale is related to the fireline intensity parameter I, which is the kinematic heat flux into the atmosphere integrated across the fireline depth (in units of $\mathrm{Km^2s^{-1}}$), and to the mixed-layer depth z_i.

We speculate that this interesting result is because smoke from a fire does not rise through a passive environment, as is often assumed for Briggs types of plume entrainment models. Instead, the fire and the environment interact in many complex ways. Some of these include: vertical-to-bent-over vortices on the ends of the fire line that rapidly mix environmental air into the buoyant smoke plume; modulation of fire intensity and fire updrafts by translation of ambient thermals across the fire line;

https://doi.org/10.5194/acp-2020-827
Preprint. Discussion started: 25 August 2020

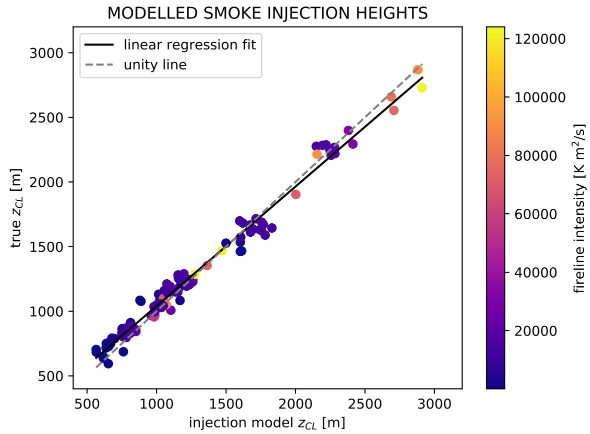

Figure 3. Comparison of true (as shown in Fig. 2) and modelled (from Eq. (8)) smoke injection heights. Scatter points represent the 140 individual plume experiments within the LES dataset, with colors corresponding to fireline intensity I. Solid black and grey dashed lines denote linear regression fit and unity, respectively.

plumes of enhanced convergence and updraft along the fire line; mass conservation as descending air beneath the extended smoke plume lowers the local mixed-layer depth; and other factors.

Thus, Eq. (1) becomes

$$g'z' = c_2 \left[\frac{I}{z_i \theta'}\right]^2 \tag{7}$$

where $c_2 = 0.5c_1$.

The above can be rearranged into the following form

$$z_{CL} - z_s = C\left[\frac{g(\theta_{CL} - \theta_s)}{\theta_s (z_{CL} - z_s)}\right]^{-\frac{1}{2}} \left\{\frac{gI(z_{CL} - z_s)}{\theta_s z_i}\right\}^{\frac{1}{3}} \tag{8}$$

where the dimensionless empirical parameter is $C \approx 1$. The factors in square and curly brackets with their corresponding powers have units of time and velocity, respectively. This relationship is plotted in Fig. 3. It provides quite an acceptable fit to the data over a wide range of 140 combinations of fire and atmospheric conditions simulated.

Equation (8) suggests that the relevant length and temperature scales (z', θ') depend not on the capping inversion strength alone, or on the tropospheric lapse rate above the capping inversion alone, but on the bulk potential-temperature differences across the smoke-plume penetration region, $z_{CL} - z_s$. Eq. (8) is implicit, in that the desired plume centerline equilibrium height z_{CL} appears in both the left and right sides of the equation. The plume centerline height also defines where θ_{CL} is retrieved from the atmospheric sounding; namely, z_{CL} is implicit in both Eq. (7) and (8). However, for any specific fire and environment conditions, values of z_{CL} are easily found by iteration (see Appendix C). Steps to estimating input parameters required for the proposed injection model from the LES data are summarized in Appendix B.

https://doi.org/10.5194/acp-2020-827
Preprint. Discussion started: 25 August 2020

Atmospheric Chemistry and Physics Discussions

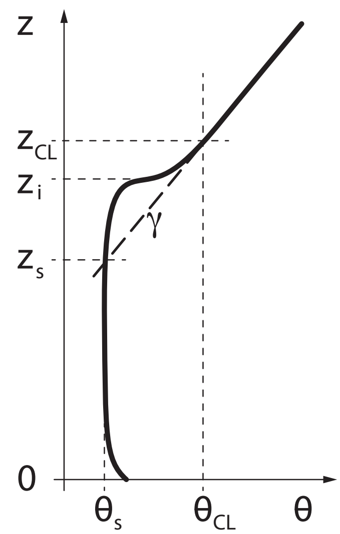

Figure 4. Idealized potential temperature profile θ vs. height with constant stable layer lapse rate γ.

Alternatively, for a small sacrifice in accuracy, we can obtain an explicit solution by considering an idealized version of the atmospheric profile, consisting of an adiabatic mixed layer, entrainment zone and a stable uniformly stratified free atmosphere above (Fig. 4). In such case γ is defined as the overall potential temperature gradient of the free atmosphere and z_s as the height corresponding to the intercept of γ and the well mixed portion of the ABL profile. Then, using Eq. (8), z_{CL} can be found explicitly as:

$$z_{CL} = C^{\frac{3}{2}} \left[\frac{\theta_s}{g}\right]^{\frac{1}{4}} \left[\frac{I}{z_i}\right]^{\frac{1}{2}} \left[\frac{1}{\gamma}\right]^{\frac{3}{4}} + z_s \tag{9}$$

4 Results

To assess the accuracy of the proposed smoke injection height parameterization (Eq. (8)), we performed two sets of verification studies. The first approach is based on using the synthetic plume dataset to perform model evaluation, bias correction and sensitivity analysis with idealized data. The second portion of this section applies our approach to a case study of a real prescribed burn (RxCADRE 2012).

4.1 Numerical Results

Shown in Fig. 3 are "true" and parameterized smoke injection heights. The former is obtained directly from the LES, as per Sect. 2.3. The latter is determined iteratively using the proposed smoke injection height parameterization (see Appendix C for implementation details).

https://doi.org/10.5194/acp-2020-827
Preprint. Discussion started: 25 August 2020

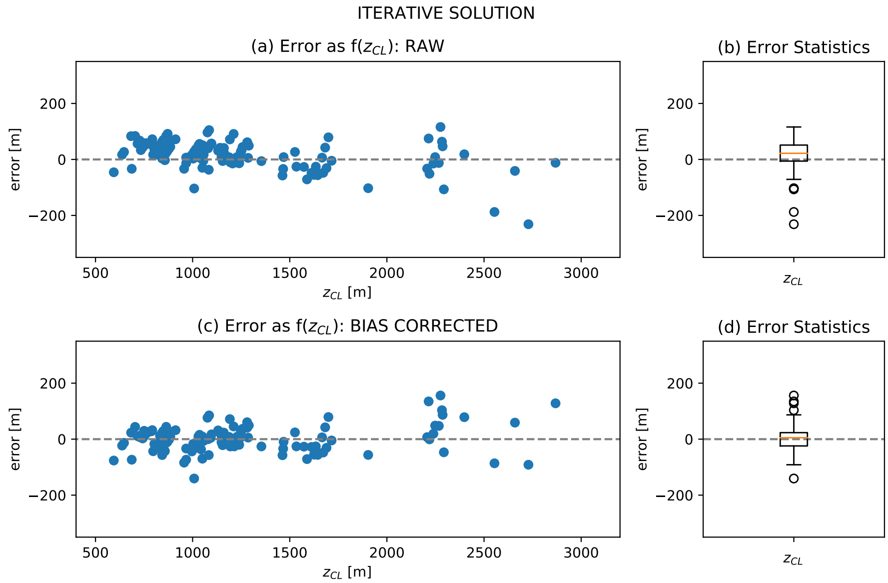

Figure 5. Performance of the smoke injection height parameterization based on the iterative solution (Eq. (8)). (a) Non-bias corrected model prediction error (true - modelled z_{CL}) as a function of z_{CL}. (b) Error statistics for non-bias corrected model. The box and whiskers span interquartile range (IQR) and 1.5 x IQR, respectively. Median value shown in orange. (c) Bias-corrected model prediction error as a function of z_{CL}. (d) Error statistics for bias-corrected model.

Individual prediction errors do not appear to be a function fireline intensity, as indicated by scatter point color in Fig. 3, or ambient winds (not shown). While overall the model performance is encouraging, the small discrepancy between the unity and regression lines suggests a linear bias. This can be remedied by applying bias correction using regression parameters from the fit shown in Fig. 3. This optimized model produces errors on the order of 20 - 30 m, as suggested by the interquartile range shown in Fig. 5d. Model bias will be addressed in further detail in Sect. 5.

Given smooth averaged profiles from the synthetic dataset and excluding condition **R8** (adiabatic free atmosphere), the explicit solution using Eq. (9) offers comparable accuracy to the iterative version for both raw and bias corrected datasets (Fig. 6) . We address the limitations of using the explicit approach in Sect. 5.4.

4.2 Model Sensitivity

To asses how sensitive the smoke injection model performance is to the particular choice of bias correction parameters, we partition our original plume dataset into training and testing groups through random sampling. We obtain the linear bias correction parameters using training data only (80% of runs). We then apply our bias-corrected iterative solution to the test group (remaining 20% of the runs) and assess model accuracy. Figure 7 summarizes model performance and sensitivity, based on 10 trials of sampling with replacement. Consistently high Pearson correlation shown in the trial histogram in Fig. 7c, are

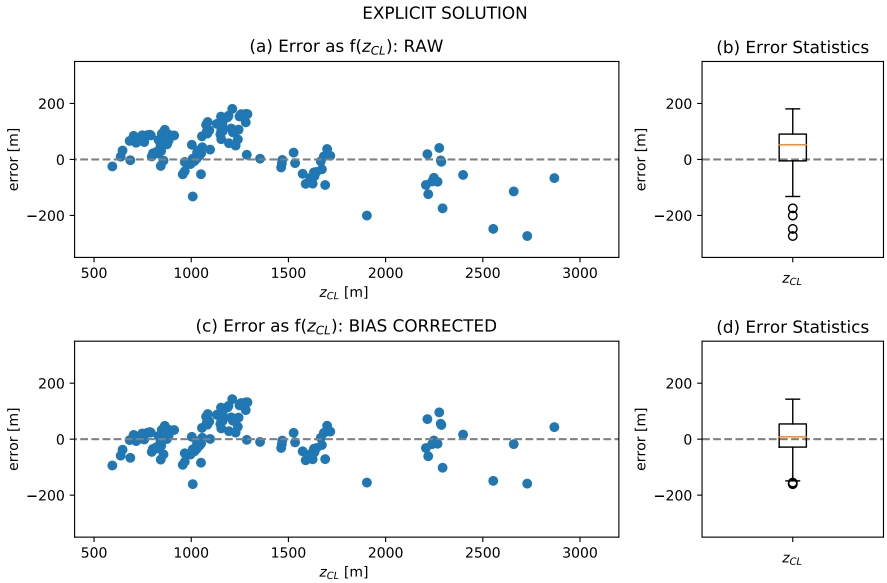

Figure 6. Performance of the smoke injection height parameterization based on the explicit solution (Eq. (9)). (a) Non-bias corrected model prediction error (true - modelled z_{CL}) as a function of z_{CL}. (b) Error statistics for non-bias corrected model. The box and whiskers span interquartile range (IQR) and 1.5 x IQR, respectively. Median value shown in orange. (c) Bias-corrected model prediction error as a function of z_{CL}. (d) Error statistics for bias-corrected model.

encouraging, and suggest that the particular choice of simulations used in bias correction does not have a strong impact on model accuracy.

4.3 Evaluation with Observations

Next, we apply the proposed model to a real-life case-study. We use observational data from the RxCADRE L2G prescribed burn (Ottmar et al., 2016) and it's numerical simulation (Moisseeva and Stull, 2019).

Shown in Fig. 8 is the strip headfire pattern used to ignite the grass lot. We estimate the burn's input fireline intensity parameter I in two different ways: from raw data collected during the burn as well as from the numerical simulation.

The observations-based value I_{obs} is derived from the integral heat flux data obtained from the Highly Instrumented Plots (HIPs) fire behavior package (FBP) sensors (Jimenez and Butler, 2016). We use the provided time-integrated values, averaging between all sensors with confirmed fire at the sensor location (as indicated by video footage (Butler et al., 2016)). We then obtain the mean value (in kinematic units) of 236 Kms^{-2} and multiply it by the average measured rate of spread (ROS) of 0.38 ms^{-1} (Butler et al., 2016) for the same sensors to convert to spatially-integrated heat flux for a single fire line. We assume that this value is representative of the remaining three firelines, hence:

$$I_{obs} = 236 \cdot 0.38 \cdot 4 = 359 \quad (10)$$

https://doi.org/10.5194/acp-2020-827
Preprint. Discussion started: 25 August 2020

Atmospheric Chemistry and Physics Discussions

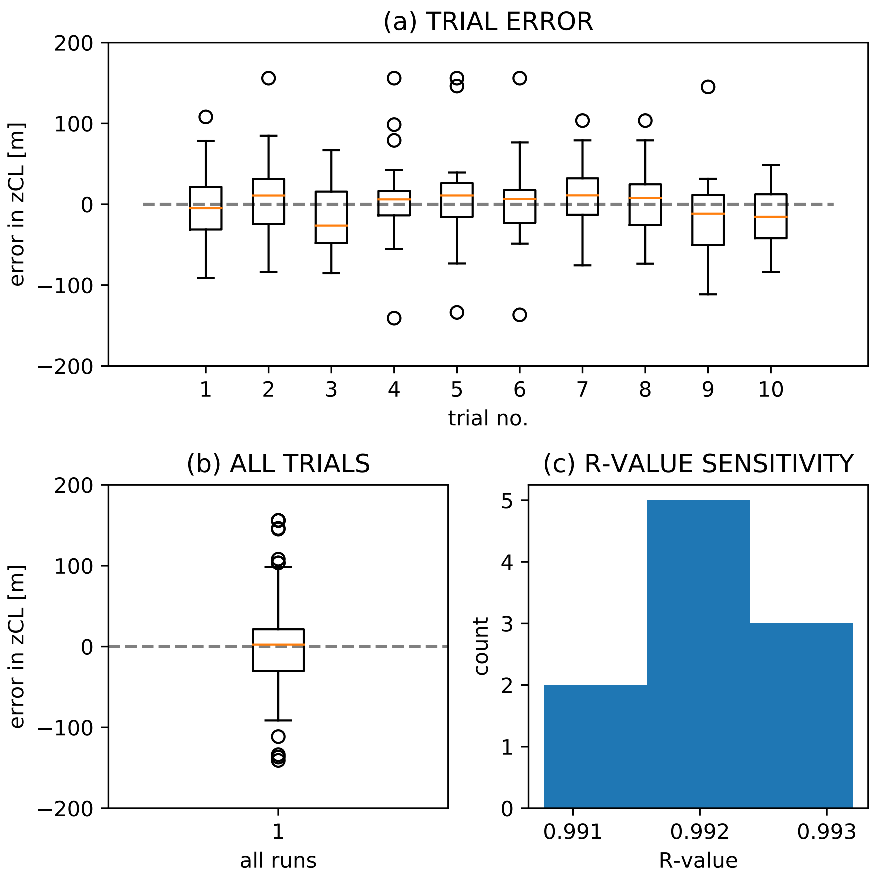

Figure 7. Analysis of model sensitivity to the choice of bias correction parameters. (a) Error distributions for individual trials using independent (test) data. (b) Error distribution for all trials using independent (test) data. (c) Sensitivity of R-value (correlation coefficient) for all trials.

in units of $\mathrm{Km^2s^{-1}}$. Note, that raw data for both heat fluxes and ROS values have extremely large associated uncertainties. Observed ROS values vary by nearly a factor of two, depending on the measurement technique used. While we have included only locations with ignition confirmed by video footage in our calculations, heat fluxes still vary up to a factor of four between sensors.

For comparison, we also obtain an LES-based integrated fireline intensity value I_{LES}. Due to wind shear, as measured by the sounding launched prior to the burn, the CWI direction at the surface differs from the one used to estimate CWI smoke. I_{LES} was, hence, estimated by assuming 125 degree rotation of LES fields, based on the lowest available wind direction measurement. We use trapezoidal rule to numerically integrate the mean crosswind heat flux along the depth of the fireline (see Appendix B) and find $I_{LES} = 1002\ \mathrm{Km^2s^{-1}}$.

Atmospheric Chemistry and Physics Discussions
Open Access
EGU

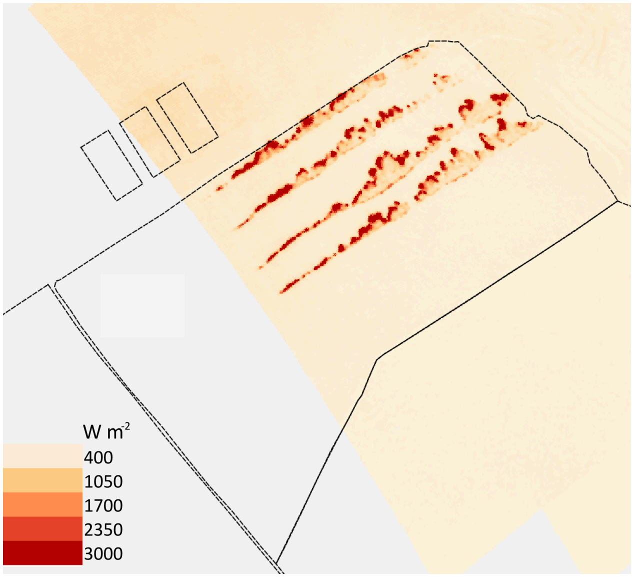

Figure 8. Long wave infra-red (LWIR) image of L2G lot during ignition (12:32:02 CST) with dashed black lines denoting burn perimeters.

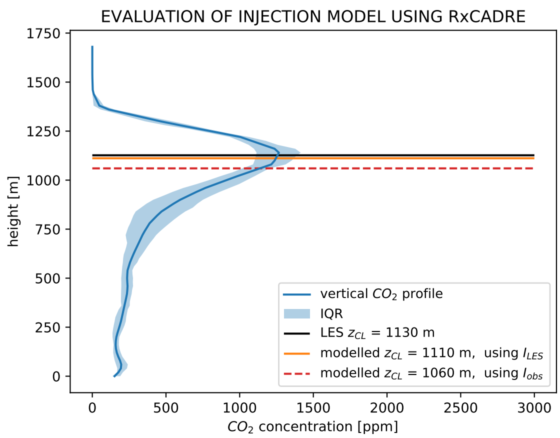

Figure 9. Model evaluation using a case-study of a real prescribed burn (RxCADRE 2012). CWI smoke concentration profile shown in blue. "True" z_{CL} obtained directly from LES shown in solid black. Solid orange and dashed red lines correspond to z_{CL} estimates obtained using the iterative solution of the proposed smoke injection height parameterization (Eq. (8)), based on LES- and observations- derived fireline intensities, respectively.

We apply our iterative solution (Eq. (8)) to find two z_{CL} estimates based on I_{obs} and I_{LES}, and compare them to the CWI smoke injection height obtained from the LES. The results are shown in Fig. 9. The parameterized injection heights are under-predicted by 20 m and 70 m for LES- and observations- derived I values, respectively.

https://doi.org/10.5194/acp-2020-827
Preprint. Discussion started: 25 August 2020

5 Discussion

5.1 Comparison with Existing Models

The above model evaluation indicates encouraging performance for the proposed smoke injection parameterization (Eq. (8)) at little computational cost. An additional advantage of our method is that it does not require making simplifying assumptions regarding the shape and heat flux distribution of the fire. This allows us to easily apply our model to complex heat sources, such as one produced with the strip head fire ignition pattern during the RxCADRE L2G prescribed burn (Fig. 8).

Unlike most existing plume rise parameterizations (Briggs, 1975; Rio et al., 2010; Freitas et al., 2007) we focus on a CWI centerline. Our model can be viewed as a "bulk method", having some common ground with the thermodynamic approach used in the FireWork modelling framework (Anderson et al., 2011; Chen et al., 2019) and the energy balance approach proposed by Sofiev et al. (2012). More specifically, we make no attempt to predict the full evolution of the rising plume centerline velocity or temperature before it reaches its equilibrium height. Rather, we focus on the energy balance of the plume over a "penetration layer".

Through analysis of the 140 LES experiments for plumes under variable fire and atmospheric conditions, we found that near-surface and boundary-layer plume dynamics are extraordinarily complex. While some aspects of plume mixing can be reasonably accounted for by making traditional entrainment assumptions, complicated features resulting from fire-atmosphere coupling, such as formation of lateral vortices and fireline wind convergence zone, are difficult to parameterize directly. Hence, we apply the energy balance approach to a layer well above the surface, starting from a reference height z_s close to the top of the ABL.

As noted in Sect. 3, the implicit functional form of our solution (Eq. (8)) can be interpreted as a characteristic timescale multiplied by the characteristic velocity scale w_f. By rearranging Eq. (7) and substituting Eq. (8) for z' it can be shown that the two expressions for w_f are equivalent, namely:

$$w_f = \left[\frac{I}{z_i\theta'}\right] = \left[\frac{gIz'}{\theta_s z_i}\right]^{\frac{1}{3}} \tag{11}$$

The scaling relationship between vertical plume velocity and cubic root of fire heat has been previously established with both Rio's and Freita's models (Rio et al., 2010; Freitas et al., 2007), although our formulation includes different variables inside the radical. While both of our forms for w_f and both model formulations (the simplified Eq. (7) and the expanded Eq. (8)) are mathematically equivalent, conversion from one form to another requires raising terms to 6^{th} power. This results in large prediction errors; hence, for practical applications, the full Eq. (8) should be used.

5.2 Dimensionless Relationship

As discussed in Sect. 3, we can obtain an explicit solution for z_{CL} by making additional assumptions about the vertical profile of potential temperature above the ABL. This allows us to reduce our Eq. (9) to a similarity relationship with two dimensionless groups $\overline{z}$ and $\overline{H}$, denoting the left hand side (LHS) and right hand side (RHS) of Eq. (12), respectively. Nondimensional $\overline{z}$ and $\overline{H}$ are linearly related, as shown in Fig. 10. The simple relationship suggests that our modelling results could fairly easily be

https://doi.org/10.5194/acp-2020-827
Preprint. Discussion started: 25 August 2020

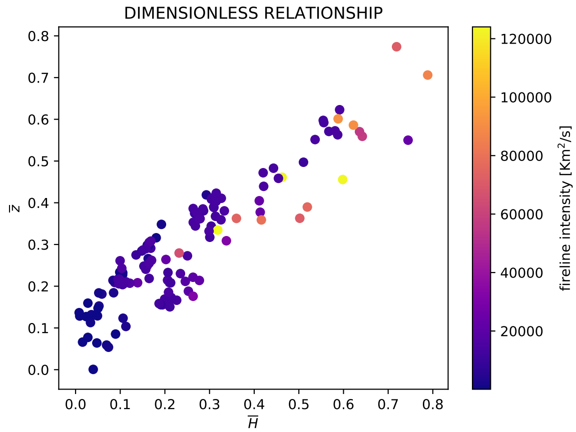

Figure 10. Similarity solution for dimensionless groups $\overline{H}$ and $\overline{z}$, corresponding to the RHS and LHS of Eq. (12), respectively. Scatter points represent individual LES runs, colored by fireline intensity parameter I.

scaled to a wider range of fire and atmospheric conditions, beyond those captured by the synthetic dataset presented in the paper.

260 $$\underbrace{\frac{z'}{z_i}}_{\overline{z}} = \underbrace{C^{\frac{3}{2}} \left[\frac{\theta_s}{g\gamma^3}\right]^{\frac{1}{4}} \left[\frac{I}{z_i^3}\right]^{\frac{1}{2}}}_{\overline{H}} \tag{12}$$

5.3 Model Bias

The raw, non-bias- corrected form of the model suffers from a positive bias for tall plumes, as suggested by Fig. 5c and 6c. In other words, z_{CL} is overpredicted for plumes injected high above the ABL. We speculate that this is due to the simplifying assumption that most of the cooling, mixing, and dilution occurs below the reference level z_s in upper portion of the ABL. As the distance between z_s and z_{CL} increases for tall plumes and as the smoke travels further into the free atmosphere, this assumption becomes increasingly less accurate. Additional radiative cooling and entrainment of ambient air is, therefore, unaccounted for, resulting in over-prediction for z_{CL}.

This issue is largely resolved for our dataset with the applied bias-correction. However, cases with strong shear turbulence and active smoke mixing above the ABL are still likely to be overestimated.

https://doi.org/10.5194/acp-2020-827
Preprint. Discussion started: 25 August 2020

5.4 Limitations

The most significant limitation of the proposed smoke injection height parameterization is that it applies only to smoke plumes with no water vapor condensation. Latent heat effects are not considered. Hence, smoke injection level for extreme pyroconvective events (e.g. flammagenitus clouds (Organization, 2017)) will likely be grossly under-predicted with the given formulation.

Another limitation is the inherently implicit form of the full model Eq. (8). While we have not encountered any issues using an iterative solver to find z_{CL}, atypical (or extremely noisy) ambient atmospheric soundings could potentially affect convergence. The explicit form (Eq. (9)) derived using the idealizing ambient sounding (Fig. 4) offers a possible solution for such cases. However, it fails for weakly stable and adiabatic free atmosphere (eg. condition R8 in Fig. 1), as θ_s is extrapolated into lower levels of ABL.

Lastly, the model has been developed and tested only for typical daytime atmospheric conditions. We have not assessed model performance for stable night-time atmospheric profiles or in the presence of strong vertical windshear.

6 Conclusions

In this study we present a simple parameterization (Eq. (8)) for predicting CWI smoke-plume centerline height from a wildfire of an arbitrary shape and intensity. We constrain and evaluate the proposed model, using a synthetic LES-derived plume dataset developed for a wide range of fire and atmospheric conditions. Based on the results of cross-evaluation with LES data as well as a real prescribed burn case study, the parameterization offers reasonable accuracy at little computational cost. We hope that the proposed approach will be of interest to air-quality researchers to provide a low-cost solution for wildfire emissions-modelling applications.

Code availability. S1: WRF-SFIRE sample initialization files (sample_simulation.zip)

Appendix A: Identifying Quasi-Stationarity

We define the quasi-stationary downwind region for each plume based on two factors: the height of the centerline and tracer concentration gradient along the centerline. Our filter attempts to extract only those portions of the downwind CWI smoke distribution, where both of these factors are changing slowly.

First, we remove the effect of random turbulent oscillations by applying a smoothing function (Savitzky-Golay filter provided by SciPy library with polynomial order set to 3) to both the concentration gradient along the centerline and the centerline height. We vary the size of the smoothing window as a function of mean ambient wind condition **W**, such that $window\_length = max(\mathbf{W} \cdot 10 + 1, 51)$ grid points.

The filter then applies the following criteria to extract quasi-stationary regions:

– smoothed tracer concentration along the plume centerline varies by less then 10% of the maximum concentration gradient

https://doi.org/10.5194/acp-2020-827
Preprint. Discussion started: 25 August 2020

Table B1. Variable descriptions and units used in smoke injection model.

Variable	**Unit**	**Description**
I	$\mathrm{Km^2s^{-1}}$	fireline integrated heat flux
g	$\mathrm{ms^{-2}}$	gravity constant = 9.81
θ_{CL}	K	ambient potential temperature at z_{CL}
θ_s	K	ambient potential temperature at z_s
z_{CL}	m	smoke injection height
z_i	m	boundary layer height
z_s	m	reference height

- smoothed centerline height varies by less then a 100 m
- the location is downwind of the maximum tracer concentration gradient
- the location is at least 10 grid points away from the maximum in smoothed and non-smoothed centerline height
- the location is at least 50 grid points away from the downwind endpoint of the centerline

The above thresholds were determined through an informal sensitivity analysis (not shown), based on the filter's ability to effectively identify regions of near-stationary plume centerline height for all simulations in our dataset.

Appendix B: Estimating Model Input Parameters

Summarized in Table B1 are parameters associated with an iterative solution for z_{CL} using Eq. (8). Below is our approach to estimating these parameters from LES data.

As noted above, we consider the problem in crosswind direction. Given a three-dimensional fire of an arbitrary shape (eg. Fig. 2b) and an ambient atmospheric sounding, we first average the fire kinematic heat flux for all ignited cells (where heat flux > 1 $\mathrm{kWm^{-2}}$) over the crosswind (y) direction at the surface (red line on Fig. 2a). Due to surface wind shear this direction may differ from the one used for calculating CWI smoke concentrations (as shown in Sect. 4.3). To obtain fireline intensity parameter I we numerically integrate the crosswind averaged heat fluxes over the depth of the fireline in the along-wind (x) direction.

We use pre-ignition potential temperature profile (i.e. the ambient environment upwind of the fire) averaged over the entire LES domain as an environmental sounding. All model fields are interpolated to have a 20 m vertical increment. z_i is defined as the height of the strongest environmental lapse rate gradient, and $z_s = \frac{3}{4} z_i$, based on informal model sensitivity analysis (not shown). The exact choice of z_s has little effect on model performance as long as it remains within the upper portion of the uniform potential temperature well-mixed layer.

https://doi.org/10.5194/acp-2020-827
Preprint. Discussion started: 25 August 2020

Atmospheric Chemistry and Physics Discussions
Open Access EGU

The values of θ_s and θ_{CL} are then determined from the pre-ignition sounding for each simulation using the definitions of z_s and z_{CL} (as described in Sect. 2.3).

Appendix C: Iterative Solution for z_{CL}

The numerical implementation of our iterative solution using SciPy's fsolve function (scipy.optimize.fsolve) is as follows. We rewrite bias corrected Eq. (8) into an input function $toSolve$ as:

$$toSolve = lambda\ z : z - B_1(z_s + C\left[\frac{g(T0[int(\frac{z}{dz})] - \theta_s)}{\theta_s(z - z_s)}\right]^{-\frac{1}{2}}\left[\frac{gI(z - z_s)}{\theta_s z_i}\right]^{\frac{1}{3}}) - B_2 \tag{C1}$$

where $C = 1.005$, $B_1 = 0.924$ and $B_2 = 116.417$ are bias correction parameters, $T0$ is the potential temperature sounding vector, dz is the vertical step and $int()$ is a standard Python function converting the bracketed value into an integer.

A possible issue for some solvers is that we are, effectively, iterating over the vertical index of the column vector $T0$ corresponding to z_{CL}. As the numerical solver attempts to converge on a solution it may query a non-existent index and fail. We are able to obtain a fast and consistent performance by ensuring we set z_i as the initial guess for z_{CL} and by minimizing the initial step bound option of the solver

$$z_{CL} = fsolve(toSolve, z_i, factor = 0.1) \tag{C2}$$

Author contributions. Conceptualization: Nadya Moisseeva and Roland Stull; methodology: Nadya Moisseeva; resources: Roland Stull; data curation: Nadya Moisseeva; writing (original draft preparation): Nadya Moisseeva and Roland Stull; writing (review and editing): Nadya Moisseeva and Roland Stull; visualization: Nadya Moisseeva; supervision: Roland Stull; funding acquisition: Nadya Moisseeva and Roland Stull

Competing interests. The authors declare that they have no conflict of interest.

Acknowledgements. We sincerely thank Dr. Rosie Howard and Chis Rodell for the countless fruitful discussions, new ideas and encouragement. We would like to acknowledge WestGrid and ComputeCanada for providing computational resources for LES runs, and Julia Jeworrek for her ongoing generous help with cluster access. Thank you to all members of UBC Weather Research and Forecasting Team for their motivation and support. This work was funded by grants from Natural Sciences and Engineering Research Council of Canada (NSERC), Natural Resources Canada (NRCan), Fraser Basin Council (BC CLEAR), British Columbia Ministry of Environment and Climate Change Strategy, Alberta Ministry of Environment and Parks and Government of the Northwest Territories.

References

Anderson, H. E.: Aids to determining fuel models for estimating fire behavior, The Bark Beetles, Fuels, and Fire Bibliography, p. 143, 1982.

Anderson, K., Pankratz, A., and Mooney, C.: 9.2 A thermodynamic approach to estimating smoke plume heights, in: Proceedings of Ninth Symposium on Fire and Forest Meteorology, Palms Springs, CA, pp. 17–21, 2011.

Briggs, G.: Plume Rise Equations, pp. 59–111, AMS: Boston, MA, USA, 1975.

Butler, B., Teske, C., Jimenez, D., O'Brien, J., Sopko, P., Wold, C., Vosburgh, M., Hornsby, B., and Loudermilk, E.: Observations of energy transport and rate of spreads from low-intensity fires in longleaf pine habitat –RxCADRE 2012, International Journal of Wildland Fire, 25, 76–89, http://dx.doi.org/10.1071/WF14154, 2016.

Chen, J., Anderson, K., Pavlovic, R., Moran, M. D., Englefield, P., Thompson, D. K., Munoz-Alpizar, R., and Landry, H.: The FireWork v2.0 air quality forecast system with biomass burning emissions from the Canadian Forest Fire Emissions Prediction System v2.03, Geoscientific Model Development, 12, 3283–3310, https://doi.org/10.5194/gmd-12-3283-2019, https://www.geosci-model-dev.net/12/3283/2019/, 2019.

Clements, C. B., Potter, B. E., and Zhong, S.: In situ measurements of water vapor, heat, and CO2 fluxes within a prescribed grass fire, International Journal of Wildland Fire, 15, 299–306, 2006.

Coen, J. L., Cameron, M., Michalakes, J., Patton, E. G., Riggan, P. J., and Yedinak, K. M.: WRF-Fire: Coupled Weather–Wildland Fire Modeling with the Weather Research and Forecasting Model, Journal of Applied Meteorology and Climatology, 52, 16–38, https://doi.org/10.1175/JAMC-D-12-023.1, http://dx.doi.org/10.1175/JAMC-D-12-023.1, 2012a.

Coen, J. L., Cameron, M., Michalakes, J., Patton, E. G., Riggan, P. J., and Yedinak, K. M.: WRF-Fire: Coupled Weather–Wildland Fire Modeling with the Weather Research and Forecasting Model, Journal of Applied Meteorology and Climatology, 52, 16–38, https://doi.org/10.1175/JAMC-D-12-023.1, http://dx.doi.org/10.1175/JAMC-D-12-023.1, 2012b.

Cushman-Roisin, B.: Atmospheric boundary layer, Environmental Fluid Mechanics, pp. 165–186, 2014.

Freitas, S. R., Carvalho, J., Longo, K., Chatfield, R., Latham, D., Silva Dias, M., Andreae, M., Prins, E., Santos, J., and Gielow, R.: Including the sub-grid scale plume rise of vegetation fires in low resolution atmospheric transport models, Atmospheric Chemistry and Physics, pp. 3385–3398, 2007.

Goodrick, S. L., Achtemeier, G. L., Larkin, N. K., Liu, Y., and Strand, T. M.: Modelling smoke transport from wildland fires: a review, International Journal of Wildland Fire, 22, 83–94, 2013.

Heilman, W. E., Liu, Y., Urbanski, S., Kovalev, V., and Mickler, R.: Wildland fire emissions, carbon, and climate: Plume rise, atmospheric transport, and chemistry processes, Forest Ecology and Management, 317, 70–79, 2014.

Ichoku, C., Kahn, R., and Chin, M.: Satellite contributions to the quantitative characterization of biomass burning for climate modeling, Atmospheric Research, 111, 1 – 28, https://doi.org/https://doi.org/10.1016/j.atmosres.2012.03.007, http://www.sciencedirect.com/science/article/pii/S0169809512000750, 2012.

Jimenez, D. and Butler, B.: RxCADRE 2012: RxCADRE 2012: In-situ fire behavior measurements, https://doi.org/https://doi.org/10.2737/RDS-2016-0038, 2016.

Kochanski, A. K., Jenkins, M. A., Mandel, J., Beezley, J. D., Clements, C. B., and Krueger, S.: Evaluation of WRF-SFIRE performance with field observations from the FireFlux experiment, Geosci. Model Dev., 6, 1109–1126, https://doi.org/10.5194/gmd-6-1109-2013, http://www.geosci-model-dev.net/6/1109/2013/, 2013.

Kochanski, A. K., Mallia, D. V., Fearon, M. G., Mandel, J., Souri, A. H., and Brown, T.: Modeling Wildfire Smoke Feedback Mechanisms Using a Coupled Fire-Atmosphere Model With a Radiatively Active Aerosol Scheme, Journal of Geophysical Research: Atmospheres, 124, 9099–9116, 2019.

Larkin, N. K., O'Neill, S. M., Solomon, R., Raffuse, S., Strand, T., Sullivan, D. C., Krull, C., Rorig, M., Peterson, J., and Ferguson, S. A.: The BlueSky smoke modeling framework, International Journal of Wildland Fire, 18, 906–920, 2010.

Mallia, D. V., Kochanski, A. K., Urbanski, S. P., and Lin, J. C.: Optimizing smoke and plume rise modeling approaches at local scales, Atmosphere, 9, 166, 2018.

Mandel, J., Amram, S., Beezley, J., Kelman, G., Kochanski, A., Kondratenko, V., Lynn, B., Regev, B., and Vejmelka, M.: Recent advances and applications of WRF–SFIRE, Natural Hazards and Earth System Sciences, 14, 2829–2845, 2014.

Moisseeva, N. and Stull, R.: Capturing Plume Rise and Dispersion with a Coupled Large-Eddy Simulation: Case Study of a Prescribed Burn, Atmosphere, 10, 579, 2019.

Organization, W. M.: International Cloud Atlas, World Meteorological Organization, https://cloudatlas.wmo.int/en/flammagenitus.html, 2017.

Ottmar, R. D., Hiers, J. K., Butler, B. W., Clements, C. B., Dickinson, M. B., Hudak, A. T., O'Brien, J. J., Potter, B. E., Rowell, E. M., Strand, T. M., and Zajkowski, T. J.: Measurements, datasets and preliminary results from the RxCADRE project –2008, 2011 and 2012, International Journal of Wildland Fire, 25, 1–9, http://dx.doi.org/10.1071/WF14161, 2016.

Paugam, R., Wooster, M., Freitas, S., and Val Martin, M.: A review of approaches to estimate wildfire plume injection height within large-scale atmospheric chemical transport models, Atmospheric Chemistry and Physics, 16, 907–925, https://doi.org/10.5194/acp-16-907-2016, https://www.atmos-chem-phys.net/16/907/2016/, 2016.

Pavlovic, R., Chen, J., Anderson, K., Moran, M. D., Beaulieu, P.-A., Davignon, D., and Cousineau, S.: The FireWork air quality forecast system with near-real-time biomass burning emissions: Recent developments and evaluation of performance for the 2015 North American wildfire season, Journal of the Air & Waste Management Association, 66, 819–841, 2016.

Prichard, S., O'Neill, S., and Urbanski, S.: Evaluation of revised emissions factors for emissions prediction and smoke management, https://www.epa.gov/sites/production/files/2017-10/documents/prichard.pdf, 2017.

Prichard, S., Larkin, N. S., Ottmar, R., French, N. H., Baker, K., Brown, T., Clements, C., Dickinson, M., Hudak, A., Kochanski, A., et al.: The Fire and Smoke Model Evaluation Experiment—A Plan for Integrated, Large Fire–Atmosphere Field Campaigns, Atmosphere, 10, 66, 2019.

Rio, C., Hourdin, F., and Chédin, A.: Numerical simulation of tropospheric injection of biomass burning products by pyro-thermal plumes, Atmospheric Chemistry and Physics, 10, https://doi.org/10.5194/acp-10-3463-2010, 2010.

Sofiev, M., Ermakova, T., and Vankevich, R.: Evaluation of the smoke-injection height from wild-land fires using remote-sensing data, Atmospheric Chemistry and Physics, 12, 1995–2006, https://doi.org/10.5194/acp-12-1995-2012, https://www.atmos-chem-phys.net/12/1995/2012/, 2012.

Val Martin, M., Logan, J. A., Kahn, R. A., Leung, F.-Y., Nelson, D. L., and Diner, D. J.: Smoke injection heights from fires in North America: analysis of 5 years of satellite observations, Atmospheric Chemistry and Physics, 10, 1491–1510, https://doi.org/10.5194/acp-10-1491-2010, https://www.atmos-chem-phys.net/10/1491/2010/, 2010.